

**ROBOTIC EXPLORATION POTENTIAL OF MARTIAN CAVES.** M. L. Kearney<sup>1</sup>, J. J. Wynne<sup>2</sup>, G. E. Cushing<sup>3</sup>, N. M. Bardabelias<sup>4</sup>, and N. G. Barlow<sup>1,5</sup>. <sup>1</sup>Department of Astronomy and Planetary Sciences, Northern Arizona University, Flagstaff, AZ; [chellykearney@gmail.com](mailto:chellykearney@gmail.com); <sup>2</sup>Department of Biological Sciences, Merriam-Powell Center for Environmental Research, Northern Arizona University, Flagstaff, AZ; [jut.wynne@nau.edu](mailto:jut.wynne@nau.edu); <sup>3</sup>USGS Astrogeology Science Center, Flagstaff, AZ; [gcushing@usgs.gov](mailto:gcushing@usgs.gov); <sup>4</sup>Lunar and Planetary Laboratory, University of Arizona, Tucson, AZ; [nmb23@lpl.arizona.edu](mailto:nmb23@lpl.arizona.edu); <sup>5</sup>deceased.

**Introduction:** Martian caves are among the best locations to search for evidence of extinct or perhaps extant life, may provide access to stable water ice deposits, and can offer a protected environment for human habitation [1]. In recognition of the emerging importance of caves on Mars, NASEM's 2019 Astrobiology Strategy recommended emphasis on research and exploration of subsurface environments [2]. Additionally, mission architectures [1] and concepts [3] were recently developed to provide recommendations for examining Martian caves for astrobiological and habitability potential (**Fig. 1**).

To date, 1,036 cave-like features have been documented on Mars [4]. Williams et al. [5] modeled cave water-ice stability on Mars and identified the most favorable regions for ice to accumulate and persist. These datasets combined were used as a first order down selection approach to identify high priority caves for exploration.

Overall, we aimed to identify the highest priority targets for a future robotic mission to a Martian cave. Specifically, we: (1) defined caves within regions of high subterranean ice accumulation; (2) calculated cave

densities per region; and, (3) identified concentrations of caves on the Martian landscape. Additionally, we provide two examples where we applied the selection criteria for targeting high priority caves for robotic exploration [6].

**Methods:** This project examined known cave locations [4] and a subterranean ice accumulation model [5] to deduce cave entrances within regions of predicted high ice accumulation. We selected a subset of these caves based on existing HiRISE imagery, which became our dataset. We then evaluated these features using a candidate selection criteria for robotic exploration [6]. These criteria include the potential for subsurface ice, access to subsurface geology, and robotic accessibility including terrain navigability and entrance configuration. Geologic and structural characteristics were determined using available geologic maps [7,8] and HiRISE images. Nearest neighbor analysis was performed to identify cave clusters. All analyses were conducted using JMARS 5.1.8 and ArcGIS 10.8.1.

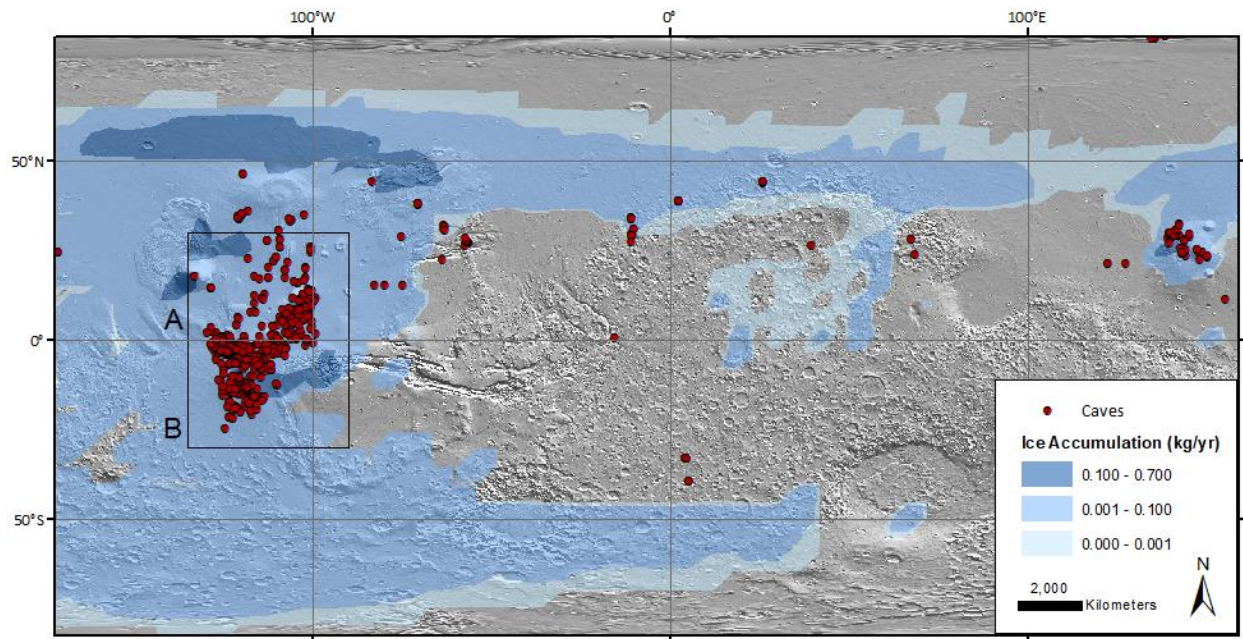


**Figure 1.** Locations of possible Martian cave entrances (red dots) [2] overlaid on the cave ice accumulation model (where predictions of annual ice mass amounts (in kg/yr) within hypothetical caves) [5] for global Mars. Areas of interest occur within the [A] Tharsis and [B] Phoenicis Lacus quadrangles. MOLA base map, courtesy NASA.

Robotic exploration potential of Martian caves: M. L. Kearney et al.

**Results:** We found 97 caves occurring within regions of high ice accumulation (0.1-0.7 kg/yr) and 847 within regions of medium accumulation (0.001-0.1 kg/yr; **Fig. 1**). The highest density (620 caves) was located within the Phoenicis Lacus quadrangle with a density of  $1.4 \times 10^{-4}$  caves/km<sup>2</sup>, while the Tharsis quadrangle was the second most dense with  $0.5 \times 10^{-4}$  caves/km<sup>2</sup> (223 caves).

HiRISE imagery is available for 28 caves, which were all within the Tharsis volcanic province. We summarized structural and geologic characteristics for these features (**Table 1**). Angular and jagged outcrops along pit rims suggestive of examinable stratigraphy was observed for 58% of the vertical features – potentially permitting robotic examination and sampling of “deep” subsurface geology. At least 23 features would permit dual-axle rover access to the entrance; this would be required for subterranean ingress of a secondary tethered rover. Most (82%) of the features were located on the lava fans and surrounding plains of Arsia Mons. Nearest neighbor analysis revealed that three features had from three to six additional features within a 25 km distance and up to 10 potential cave entrances within a 50 km radius; clusters will provide greater flexibility as multiple features could then be closely scrutinized if aerial drone technologies are employed.

While 28 features are currently being evaluated for their exploration potential, we provide preliminary results for two features as examples. The first feature is a possible skylight situated on the southern lava fan of Arsia Mons (**Fig. 2A**). Angular protrusions suggestive of viewable stratigraphy are situated along the eastern rim. Access could be gained via a drone or tethered rover. We cannot discern whether a lateral entrance is associated with this feature, which is a key requirement for robotic exploration.

Our second feature is probably not viable as it is an isolated feature occurring at an elevation of 20,244 m within Caldera V [*sensu* 9], the southernmost caldera of Olympus Mons. However, this is presently the only feature suggestive of laterally-trending passage for which HiRISE imagery is available. Located within the

southeastern wall of the caldera, the feature is likely a conduit related to the caldera, possibly a vent.

**Conclusions:** While our work will ultimately involve a thorough examination of all 28 potential cave entrances, we have provided examples of how the selection criteria will be applied. Ultimately, we will examine and quantify the robotic exploration (as well as human use) potential for all features using geospatial techniques. Caves occurring within clusters will be further examined and recommendations will likely be made for additional HiRISE imagery acquisition.

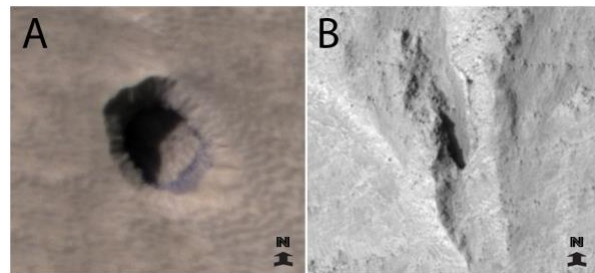


**Figure 2.** [A] Skylight on southern lava fan on Arsia Mons, diameter ~30 m (HiRISE ESP\_042942\_1680). [B] Possible laterally trending feature on Olympus Mons, length of apparent entrance, north to south, is ~10 m (HiRISE ESP\_007669\_1980).

**References:** [1] Titus, T.N. et al. (2020) *Planetary Caves Decadal Survey white paper*. [2] NASEM (2019) doi:10.177226/25252. [3] Phillips-Lander et al. (2020) *MACIE Decadal Survey white paper*. [4] Cushing, G.E. (2017) Mars Global Cave Candidate Catalog (MGC<sub>3</sub>), PDS Archive. [5] Williams, K. et al. (2010) *Icarus* 209: 358–368. [6] Wynne, J.J. et al. (2014) *NASA JPL Planetary Cave Workshop white paper*. [7] Masursky, H. et al. (1978) *USGS Mars Geologic Map of the Phoenicis Lacus Quadrangle*. [8] Scott, D. & J. Zimelman. (1996) *USGS Geologic Map of Arsia Mons*. [9] Neukum, G. et al. (2004) *Nature* 432: 971-979.

|                                 | <i>Lava Fans and Surrounding Plains of Arsia Mons</i> |       |     |     |      | <i>Caldera and Flanks of Shield - Volcanoes</i> |     |     |     | <i>Cliff</i> |
|---------------------------------|---|-------|-----|-----|------|---|-----|-----|-----|--------------|
| <b>Cave category</b>            | APC   | Sky   | Crk | End | Irr  | APC   | Rim | SRP | Lat | Irr          |
| <b>Number of caves/Category</b> | 12  | 5     | 3   | 1   | 2    | 1   | 1   | 1   | 1   | 1            |
| <b>Diameter (m)</b>             | 105-250   | 4-460 | -   | 92  | 5-40 | 170   | 60  | 45  | -   | 12           |
| <b>Elevation (m)</b>            | 6,296 - 12,330  |       |     |     |      | 14,477 - 20,244                                 |     |     |     | 4,739        |
| <b>Entrance type</b>            | All vertical  |       |     |     |      | 3 vertical, 1 lateral                           |     |     |     | Vertical     |
| <b>Visible stratigraphy</b>     | 6   | 3     | -   | -   | -    | 1   | -   | 1   | -   | -            |

**Table 1.** Geologic and structural characteristics of the 28 caves with HiRISE imagery. Cave types: atypical pit crater (APC), crack (Crk), skylight (Sky), irregularly shaped feature (Irr), entrance to rim of caldera (Rim), small rimless pit (SRP), laterally trending entrance (Lat), and pit in the end of a trough (End) [4].